.

Parametric decay of a parallel propagating monochromatic whistler wave: Particle-in-cell simulations

Yangguang Ke, Xinliang Gao, Quanming Lu, and Shui Wang

Citation: Phys. Plasmas **24**, 012108 (2017); doi: 10.1063/1.4974160
View online: http://dx.doi.org/10.1063/1.4974160
View Table of Contents: http://aip.scitation.org/toc/php/24/1
Published by the American Institute of Physics

PHYSICS OF PLASMAS 24, 012108 (2017)

Parametric decay of a parallel propagating monochromatic whistler wave: Particle-in-cell simulations

Yangguang Ke,[1,2] Xinliang Gao,[1,2,a)] Quanming Lu,[1,2] and Shui Wang[1,2]
[1]CAS Key Laboratory of Geospace Environment, Department of Geophysics and Planetary Science, University of Science and Technology of China, Hefei 230026, China
[2]Collaborative Innovation Center of Astronautical Science and Technology, Harbin 150001, China

(Received 31 October 2016; accepted 2 January 2017; published online 18 January 2017)

In this paper, by using one-dimensional (1-D) particle-in-cell simulations, we investigate the parametric decay of a parallel propagating monochromatic whistler wave with various wave frequencies and amplitudes. The pump whistler wave can decay into a backscattered daughter whistler wave and an ion acoustic wave, and the decay instability grows more rapidly with the increase of the frequency or amplitude. When the frequency or amplitude is sufficiently large, a multiple decay process may occur, where the daughter whistler wave undergoes a secondary decay into an ion acoustic wave and a forward propagating whistler wave. We also find that during the parametric decay a considerable part of protons can be accelerated along the background magnetic field by the enhanced ion acoustic wave through the Landau resonance. The implication of the parametric decay to the evolution of whistler waves in Earth's magnetosphere is also discussed in the paper. *Published by AIP Publishing.* [http://dx.doi.org/10.1063/1.4974160]

I. INTRODUCTION

Whistler-mode waves are important electromagnetic emissions in the Earth's magnetosphere, which have been commonly believed to account for both the source of relativistic ($\sim$MeV) electrons in the Van Allen radiation belt[1–3] and the precipitation of low-energy ($\sim$10 keV) electrons into the Earth's atmosphere.[4–6] In the past four decades, the whistler waves in the Earth's magnetosphere have been thoroughly studied in the linear or quasi-linear frame, which has provided a better understanding of satellite observations. However, nonlinear physical phenomena related to whistler waves are also becoming a hot topic. The well-known frequency chirping of chorus waves has been believed to be caused by nonlinear interactions between whistler waves and resonant electrons.[7,8] Lower band cascade, involving the nonlinear wave-wave coupling process, is proposed to be a potential generation mechanism for multiband chorus waves observed by THEMIS satellites.[9]

Moreover, based on observations by Van Allen Probes, Agapitov *et al.*[10] reported an event of the parametric decay of whistler waves, where the whistler waves decayed into backward daughter whistler waves and electron acoustic waves, and the generated electron acoustic waves are considered as a source of electron scale nonlinear electrostatic structures. More generally, the parametric decay of a whistler wave usually involves a backward daughter whistler wave and an ion acoustic wave, which has been studied in many previous works.[11–13] The parametric decay of a whistler wave was first proposed by Forslund *et al.*,[11] which could occur in a wide range of plasma parameters. Due to the heavy Landau damping of ion acoustic waves by ions when $T_e \leq T_i$, the parametric decay is typically considered in a plasma with $T_e \gg T_i$, where T_e and T_i are the electron and proton temperatures, respectively. However, Shukla[14] pointed out that the parametric decay of a nonparallel whistler wave even occurs in a plasma with $T_e \approx T_i$, which will involve an ion quasimode instead of the ion acoustic wave. The parametric decay of whistler waves has also been observed in laboratory plasma experiments.[15]

However, there is still a lack of studies about the parametric decay of a whistler wave in a self-consistent simulation model. Recently, Umeda *et al.*[16] studied the electron acceleration during the parametric decay of a parallel propagating monochromatic whistler wave by using a one-dimensional (1-D) particle-in-cell (PIC) model. However, in their simulation, the pump whistler wave is chosen to have an extremely high frequency (close to Ω_e, where Ω_e is the electron cyclotron frequency) and a quite large magnetic amplitude ($\sim$0.32 B_0, where B_0 is the background magnetic field). In this paper, with 1-D PIC simulation models, we have investigated the parametric decay of a parallel propagating whistler wave with various frequencies and amplitudes. The effects of the wave frequency and amplitude on the parametric decay have been studied. Meanwhile, we also consider ion dynamics during the parametric decay. The paper is organized as follows. Sec. II describes the simulation model and initial setup. Sec. III presents simulation results. At last, conclusion and discussions are given in Sec. IV.

II. SIMULATION MODEL

To study the parametric decay of a parallel propagating whistler wave, we employ a 1-D PIC simulation model with the periodic boundary condition. This model includes full three-dimensional electromagnetic fields and velocities, but only allows spatial variations in the x direction. The

a)Author to whom correspondence should be addressed. Electronic mail: gaoxl@mail.ustc.edu.cn

TABLE I. Simulation parameters for Runs 1–5.

Run	ω_0/Ω_e	$k_0/(V_{Ae}\Omega_e^{-1})^{-1}$	$\delta B/B_0$	L_x/λ_0[a]
1	0.1	0.334	0.05	5
2	0.3	0.657	0.03	10
3	0.3	0.657	0.05	10
4	0.3	0.657	0.07	10
5	0.5	1.005	0.05	15

[a]The L_x is the length of the simulation system, and the λ_0 is the wavelength of the pump wave.

background magnetic field is directed along the x axis. This system is initialized with a monochromatic pump whistler wave, which propagates along the background magnetic field $\mathbf{B}_0$. The corresponding fluctuating magnetic fields δB, electric fields δE, and transverse bulk velocities of electrons U_e are described as below[17]

$$\delta B = \delta B_y + i\delta B_z = \delta B i e^{-i\phi}, \tag{1}$$

$$\delta E = \delta E_y + i\delta E_z = \frac{\omega_0}{k_0}\delta B e^{-i\phi}, \tag{2}$$

$$U_e = -\frac{\omega_0}{k_0}\frac{\delta B}{B_0}\frac{\Omega_e}{\omega_0 - \Omega_e} i e^{-i\phi}, \tag{3}$$

where k_0 is the wave number of the pump wave, ω_0 is the wave frequency, and $\phi = k_0 x - \omega_0 t$. δB_y (δE_y) and δB_z (δE_z) are y and z components of fluctuating magnetic (electric) fields, respectively. The dispersion relation of the pump whistler wave is expressed as

$$k_0 = \frac{\omega_0}{c}\left[1 - \frac{\omega_{pe}^2}{\omega_0^2(1 - \Omega_e/\omega_0)}\right]^{1/2}, \tag{4}$$

where ω_{pe} is the electron plasma frequency, and c is the speed of light.

In simulations described below, the ratio of electron plasma frequency to electron cyclotron frequency is set as $\omega_{pe}/\Omega_e = 5$. A smaller mass ratio of proton to electron $m_i/m_e = 100$ is chosen just for reducing computational cost. The velocity distributions of electrons and protons are both Maxwellian. The electron thermal velocity is $V_{te} = 0.2V_{Ae}$ (where $V_{Ae} = \sqrt{B_0/\mu_0 N_e m_e}$), and the electron-to-ion temperature ratio is $T_e/T_i = 16$. The grid cell size and time step are $\Delta x = 0.02V_{Ae}\Omega_e^{-1}$ and $\Delta t = 0.002\Omega_e^{-1}$, respectively. There are about 100 superparticles in every cell for each component (proton or electron). Some other parameters for five simulation runs are listed in Table I.

III. SIMULATION RESULTS

The overview of the parametric decay of the pump whistler wave is shown in Fig. 1, which presents the temporal evolution of (left) forward propagating magnetic fluctuations $\delta B^+/B_0$, (middle) backward propagating magnetic fluctuations $\delta B^-/B_0$, and (right) the proton density fluctuations $\delta N_i/N_0$ for Run 3, respectively. For separating the magnetic fluctuations of the pump and daughter whistler waves, we decompose magnetic fluctuations into positive and negative helical parts following the method developed by Terasawa *et al.*[18] For a right-hand polarized whistler wave, the negative helical part corresponds to a backward propagating wave, whereas the positive helical part corresponds to a forward propagating wave. In the left panel, it clearly shows that the pump whistler wave propagates in the $+x$ direction with a phase velocity of $v_p \approx 0.46V_{Ae}$, which is consistent with the initial set up ($\omega_0/k_0 \sim 0.456V_{Ae}$). Besides, there is a clear trend that the amplitude of the pump wave decreases with the time. Meanwhile, a backward propagating whistler wave begins to grow from the noise level, which has almost the same phase velocity as the pump whistler wave (middle panel). Simultaneously, the ion density fluctuation also grows and gradually evolves into an ion density mode as

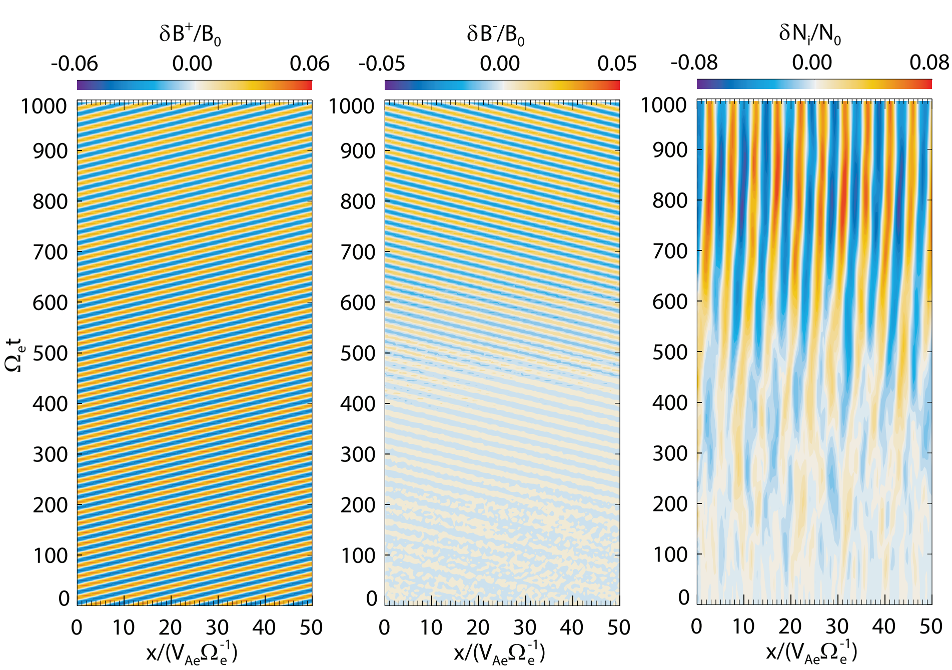

FIG. 1. Temporal evolution of (left) forward propagating magnetic fluctuations $\delta B^+/B_0$, (middle) backward propagating magnetic fluctuations $\delta B^-/B_0$ decomposed by the method developed by Terasawa *et al.*,[18] and (right) the proton density fluctuations $\delta N_i/N_0$ for Run 3.

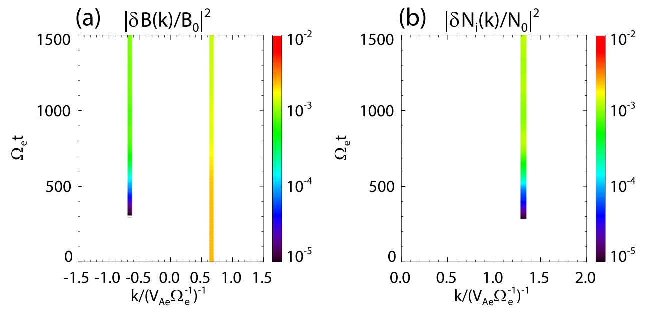

FIG. 2. Temporal evolution of the spectrum for (a) magnetic fluctuations $\delta B(k)/B_0$ and (b) ion density fluctuations $\delta N_i(k)/N_0$ for Run 3.

shown in the right panel. Here, this ion density mode is considered as the ion acoustic wave, whose phase velocity is estimated at about 0.006 V_{Ae}. As supplementary evidence, we change the mass ratio m_i/m_e from 100 to 400 and 1600 in this simulation run and find that the phase velocities of the ion density mode are reduced to $\sim$0.004 V_{Ae} and $\sim$0.0017 V_{Ae}, which suggests that the ion density mode should be the ion acoustic wave.

The temporal evolution of the spectra for (a) magnetic fluctuations and (b) ion density fluctuations is illustrated in Fig. 2 for Run 3. Initially, as shown in Fig. 2(a), there is only a pump whistler wave in the system with the wave number $k_0 \approx 0.66(V_{Ae}\Omega_e^{-1})^{-1}$. As the time increases, the backward propagating whistler wave shows up at about $\Omega_e t = 400$ and saturates at about $\Omega_e t = 800$ (Fig. 2(a)), whose wave number is about $k_1 \approx -0.66(V_{Ae}\Omega_e^{-1})^{-1}$. The ion acoustic wave begins to grow along with the increase of the backward daughter wave, and its wave number is found to be $k_2 \approx 1.32(V_{Ae}\Omega_e^{-1})^{-1} \approx 2k_0$ (Fig. 2(b)). This result is quite consistent with the theoretical prediction.[12] Moreover, the wave numbers of these three wave modes satisfy the resonant condition very well, i.e., $k_0 = k_1 + k_2$. Since the frequency of the daughter wave is nearly the same as that of the pump wave and the frequency of the ion acoustic wave can be negligible due to its very small phase velocity, their frequencies also approximately satisfy the resonant condition of $\omega_0 = \omega_1 + \omega_2$. These results demonstrate that the pump whistler wave is unstable to decay into a backward propagating daughter whistler wave and an ion acoustic wave.

The effects of wave amplitudes and frequencies on the parametric decay of a whistler wave are also considered. Figure 3 displays time profiles of amplitudes of the pump wave (solid black), daughter wave (dashed black), and ion acoustic wave (solid blue) for (a) Run 2, (b) Run 3, and (c) Run 4, respectively. In the three runs, the amplitude $\delta B/B_0$ of the pump whistler wave is initially given as 0.03, 0.05, and 0.07, respectively, but the wave frequency is kept as

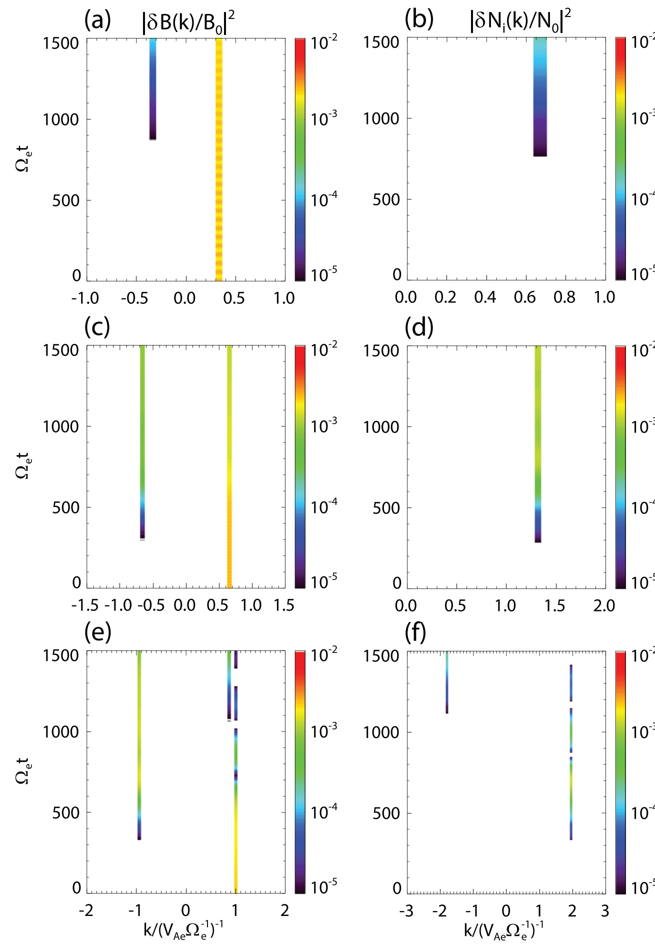

FIG. 4. Temporal evolution of the spectrum for (a) magnetic fluctuations $\delta B(k)/B_0$ and (b) ion density fluctuations $\delta N_i(k)/N_0$ for Run 1, (c) and (d) for Run 3, while (e) and (f) are for Run 5.

$\omega_0 = 0.3\Omega_e$. As shown in Fig. 3, there is a clear trend that the parametric decay of a whistler wave with a larger amplitude will occur earlier and grow more rapidly. The backward propagating whistler wave (or the ion acoustic wave) in Runs 2–4 starts to grow at $\Omega_e t \approx$ 1000, 400, and 300, respectively. Besides, we also estimate growth rates of the decay instability for Runs 2–4 by employing the linear least squares method during the linear growth phase, which are about 0.0035 Ω_e, 0.0072 Ω_e, and 0.0013 Ω_e, respectively. Note that wave numbers of generated daughter whistler waves are almost the same for the three runs (not shown here). The growth rates of theoretical calculation are 0.0055 Ω_e, 0.0093 Ω_e, and 0.013 Ω_e, respectively.

In order to investigate the effects of wave frequencies on the decay instability, we compare the results of Runs 1, 3, and 5, where pump whistler waves have different frequencies but

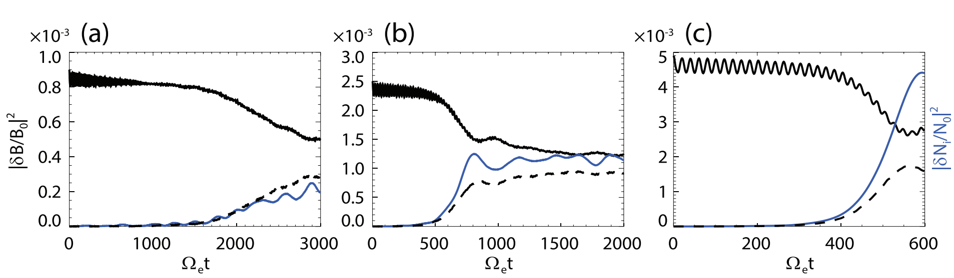

FIG. 3. Time profiles of amplitudes of the pump wave (solid black), daughter wave (dashed black), and ion acoustic wave (solid blue) for (a) Run 2, (b) Run 3, and (c) Run 4, respectively.

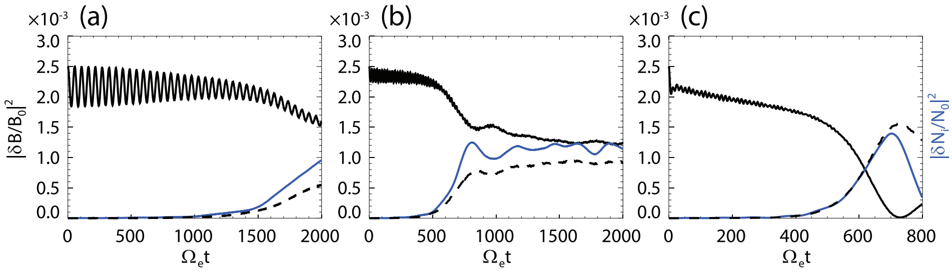

FIG. 5. Time profiles of amplitudes of the pump wave (solid black), daughter wave (dashed black), and ion acoustic wave (solid blue) for (a) Run 1, (b) Run 3, and (c) Run 5, respectively.

the same amplitude. Figures 4(a) and 4(b) display the temporal evolution of the spectrum for magnetic fluctuations $\delta B/B_0$ and ion density fluctuations $\delta N_i/N_0$ for Run 1, Figs. 4(c) and 4(d) for Run 3, while Figs. 4(e) and 4(f) are for Run 5. As shown in Figs. 4(a) and 4(b), the pump whistler wave with $k_0 \approx 0.33(V_{Ae}\Omega_e^{-1})^{-1}$ decays into a backward propagating whistler wave with the wave number $k_1 \approx -k_0$ and an ion acoustic wave with the wave number $k_2 \approx 2k_0$, which is quite similar to the decay process shown in Fig. 2 for Run 3. Interestingly, we observe a multiple decay process for Run 5 in Figs. 4(e) and 4(f). Before $\Omega_e t \approx 1100$, the pump whistler wave with $k_0 \approx 1.0(V_{Ae}\Omega_e^{-1})^{-1}$ decays into a backward propagating whistler wave with $k_1 \approx -0.95(V_{Ae}\Omega_e^{-1})^{-1}$ and a forward propagating ion acoustic wave with $k_2 \approx 1.95(V_{Ae}\Omega_e^{-1})^{-1}$, and they satisfy the resonant condition (i.e., $k_0 = k_1 + k_2$). However, since the excited daughter whistler wave has a sufficiently large amplitude, it is also unstable to the parametric decay. As a result, a third forward propagating whistler wave with $k_3 \approx 0.87(V_{Ae}\Omega_e^{-1})^{-1}$ appears from $\Omega_e t \approx 1100$ along with the occurrence of a backward propagating ion acoustic wave with $k_4 \approx -1.82(V_{Ae}\Omega_e^{-1})^{-1}$. The resonant condition (i.e., $k_1 = k_3 + k_4$) is also satisfied, which supports the parametric decay of the backward propagating daughter whistler wave.

Figure 5 presents time profiles of amplitudes of the pump wave (solid black), daughter wave (dashed black), and ion acoustic wave (solid blue) for (a) Run 1, (b) Run 3, and (c) Run 5, respectively. The parametric decay of the pump wave with $\omega_0 = 0.1\Omega_e$, $0.3\Omega_e$, and $0.5\Omega_e$ is observed to take place at $\Omega_e t \approx 1000$, 400, and 300, respectively, as shown in Figs. 5(a)–5(c). Besides, we also estimate growth rates for Runs 1, 3, and 5, which are 0.0033 Ω_e, 0.0072 Ω_e, and 0.012 Ω_e, respectively. And the theoretically calculated growth rates are 0.0043 Ω_e, 0.0093 Ω_e, and 0.013 Ω_e, respectively.

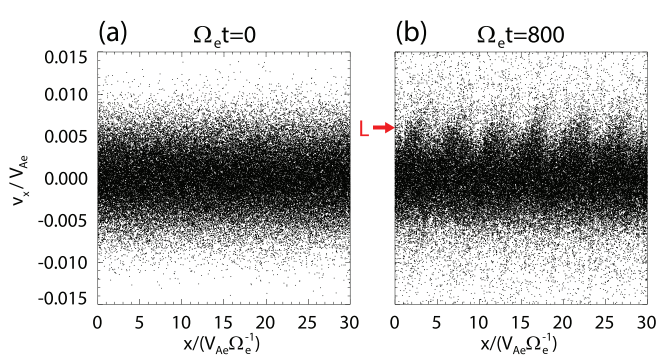

FIG. 6. Scatter plots of protons in the $x - v_x$ phase space for Run 3 at (a) $\Omega_e t = 0$ and (b) $\Omega_e t = 800$, respectively. The red arrow marks the value of the Landau resonant velocity.

As a summary, we can find that with the increase of the frequency of the pump whistler wave, the parametric decay will take place earlier, and the growth rate of this instability will become larger.

The proton dynamics during the parametric decay of the whistler wave are also studied. Figure 6 describes scatter plots of protons in the $x - v_x$ phase space for Run 3 at (a) $\Omega_e t = 0$ and (b) $\Omega_e t = 800$, respectively. Initially, protons have a Maxwellian velocity distribution with $V_{ti} = 0.005V_{Ae}$, and there is no bulk velocity along the background magnetic field (Fig. 6(a)). However, at $\Omega_e t = 800$, just after the saturation of the parametric decay, the deformation of the proton parallel velocity distribution is obvious as shown in Fig. 6(b). There is a considerable part of protons accelerated along the background magnetic field through the Landau resonance due to the enhanced ion acoustic wave. The phase velocity of the generated ion acoustic wave is estimated to be about 0.006 V_{Ae}, making the Landau resonance easily satisfied for protons.

IV. CONCLUSIONS AND DISCUSSION

By employing 1-D PIC simulations, we have studied the parametric decay of the parallel propagating monochromatic whistler wave with various wave frequencies and amplitudes. In our simulations, the pump whistler wave will decay into a backward propagating daughter whistler wave and an ion acoustic wave. Besides, there is a clear trend that the parametric decay of the whistler wave will take place earlier and grow more rapidly with the increase of the wave frequency/amplitude. We also find a multiple decay process for a pump wave with sufficiently high frequency or large amplitude, where the generated daughter whistler is also unstable to the parametric decay. Besides, during the parametric decay, a considerable part of protons can be accelerated along the background magnetic field by the enhanced ion acoustic wave through the Landau resonance.

We have also compared growth rates estimated in simulations with those obtained from the theoretical calculation. The growth rates of the decay instability for Runs 2–4 are about 0.0035 Ω_e, 0.0072 Ω_e, and 0.013 Ω_e, respectively, while the theoretical growth rates are 0.0055 Ω_e, 0.0093 Ω_e, and 0.013 Ω_e, respectively.[11] Besides, we also estimate growth rates for Runs 1, 3, and 5, which are 0.0033 Ω_e, 0.0072 Ω_e, and 0.012 Ω_e, respectively. And the theoretically calculated growth rates are 0.0043 Ω_e, 0.0093 Ω_e, and 0.013 Ω_e, respectively.[11] In this study, the maximum growth rate of the excited ion acoustic wave is used to represent the growth rate of the decay instability. According to the theory, the maximum growth rate of the excited ion acoustic wave at the frequency ω_s is given as $\gamma = \omega_0(\alpha\omega_0/\omega_s)^{1/2}$, where $\alpha \equiv (\Omega_i/\omega_0)\delta B^2/B_0^2$, $\omega_s = 2k_0(T_e/m_i)^{1/2}$, and Ω_i is the ion cyclotron frequency.[11] The clear trend that the growth rate of the parametric decay will increase with the increase of the wave frequency/amplitude is quite consistent with theoretical results. Note that growth rates obtained from our simulations are slightly smaller than theoretical ones, which may be due to the damping of ion acoustic waves in the self-consistent simulation.[11]

The nonlinear evolution of whistler waves in the Earth's magnetosphere is beginning to attract more and more attention. Based on observations by Van Allen Probes, Agapitov *et al.*[10] reported an event of the parametric decay of whistler waves, where the whistler wave decays into a backward daughter whistler wave and an electron acoustic wave. Gao *et al.*[9] reported two multiband chorus waves and proposed a new generation mechanism of upper band chorus waves, named as the lower band cascade, which involves the wave-wave coupling between lower band chorus waves and density fluctuations caused by fluctuating electric fieds along the wave vector of lower band chorus. According to our simulations, the parametric decay involving the ion acoustic wave may be also a potential physical process during the evolution of whistler waves in the Earth's magnetosphere. Note that, we only consider the parametric decay of whistler waves in a plasma with $T_e \gg T_i$, which is due to the heavy Landau damping of ion acoustic waves by ions when $T_e \leq T_i$. In this paper, we only investigate the parametric decay of the parallel propagating whistler wave, but whistler waves in the magnetosphere typically have a finite wave normal angle. Studying the parametric decay of nonparallel whistler waves should require a two-dimensional simulation model, and it will be left for a future work.

ACKNOWLEDGMENTS

The authors express their thanks for the valuable discussion with M. Y. Yu at Zhejiang University. The work was supported by the NSFC Grant Nos. 41604128, 41631071, 41474125, 41331067, and 41421063, Fundamental Research Funds for the Central Universities, Key Research Program of Frontier Sciences, CAS (QYZDJ-SSW-DQC010), and Youth Innovation Promotion Association of Chinese Academy of Sciences (No. 2016395).

[1]G. D. Reeves, H. E. Spence, M. G. Henderson, S. K. Morley, R. H. W. Friedel, H. O. Funsten, D. N. Baker, S. G. Kanekal, J. B. Blake, J. F. Fennell, S. G. Claudepierre, R. M. Thorne, D. L. Turner, C. A. Kletzing, W. S. Kurth, B. A. Larsen, and J. T. Niehof, Science **341**, 991 (2013).
[2]R. M. Thorne, W. Li, B. Ni, Q. Ma, J. Bortnik, L. Chen, D. N. Baker, H. E. Spence, G. D. Reeves, M. G. Henderson, C. A. Kletzing, W. S. Kurth, G. B. Hospodarsky, J. B. Blake, J. F. Fennell, S. G. Claudepierre, and S. G. Kanekal, Nature **504**, 411 (2013).
[3]D. Mourenas, A. V. Artemyev, O. V. Agapitov, V. Krasnoselskikh, and W. Li, J. Geophys. Res. **119**, 9962, doi:10.1002/2014JA020443 (2014).
[4]R. M. Thorne, B. Ni, X. Tao, R. B. Horne, and N. P. Meredith, Nature **467**, 943 (2010).
[5]B. Ni, R. M. Thorne, N. P. Meredith, Y. Y. Shprits, and R. B. Horne, J. Geophys. Res. **116**, A10207, doi:10.1029/2011JA016517 (2011).
[6]Y. Nishimura, J. Bortnik, W. Li, R. M. Thorne, B. Ni, L. R. Lyons, V. Angelopoulos, Y. Ebihara, J. W. Bonnell, O. L. Contel, and U. Auster, J. Geophys. Res. **118**, 664, doi:10.1029/2012JA018242 (2013).
[7]Y. Omura, Y. Katoh, and D. Summers, J. Geophys. Res. **113**, A04223, doi:10.1029/2007JA012622 (2008).
[8]X. Gao, W. Li, R. M. Thorne, J. Bortnik, V. Angelopoulos, Q. Lu, X. Tao, and S. Wang, Geophys. Res. Lett. **41**, 4805, doi:10.1002/2014GL060707 (2014).
[9]X. Gao, Q. Lu, J. Bortnik, W. Li, L. Chen, and S. Wang, Geophys. Res. Lett. **43**, 2343, doi:10.1002/2016GL068313 (2016).
[10]O. V. Agapitov, V. Krasnoselskikh, F. S. Mozer, A. V. Artemyev, and A. S. Volokitin, Geophys. Res. Lett. **42**, 3715, doi:10.1002/2015GL064145 (2015).
[11]D. W. Forslund, J. M. Kindel, and E. L. Lindman, Phys. Rev. Lett. **29**, 249 (1972).
[12]K. F. Lee, Phys. Fluids **17**, 1343 (1974).
[13]P. K. Shukla, M. Y. Yu, and K. H. Spatschek, Phys. Fluids **18**, 265 (1975).
[14]P. K. Shukla, Phys. Rev. A **16**, 1294 (1977).
[15]M. Porkolab, V. Arunasalam, and R. A. Ellis, Jr., Phys. Rev. Lett. **29**, 1438 (1972).
[16]T. Umeda, S. Saito, and Y. Nariyuki, Astrophys. J. **794**, 63 (2014).
[17]S. Saito, Y. Nariyuki, and T. Umeda, Phys. Plasmas **22**, 072105 (2015).
[18]T. Terasawa, M. Hoshino, J.-I. Sakai, and T. Hada, J. Geophys. Res. **91**, 4171, doi:10.1029/JA091iA04p04171 (1986).